Biochimica et Biophysica Acta, 723 (1983) 350–357
Elsevier

BBA 41299

THE LOCATION OF REDOX CENTERS IN THE PROFILE STRUCTURE OF A RECONSTITUTED MEMBRANE CONTAINING A PHOTOSYNTHETIC REACTION CENTER-CYTOCHROME *c* COMPLEX BY RESONANCE X-RAY DIFFRACTION

J.K. BLASIE [a,b], J.M. PACHENCE [a,b,*], A. TAVORMINA [a,b], P.L. DUTTON [b], J. STAMATOFF [c,**], P. EISENBERGER [c,***] and G. BROWN [d]

Department of [a] Chemistry and [b] Biochemistry-Biophysics, University of Pennsylvania, Philadelphia, PA, [c] Bell Telephone Laboratories, Murray Hill, NJ and [d] Stanford Synchrotron Radiation Laboratory, Stanford, CA (U.S.A.)

(Received November 1st, 1982)
(Revised manuscript received February 22nd, 1983)

Key words: Redox center localization; Reaction center-cytochrome c complex; Photosynthesis; Membrane reconstitution; Resonance X-ray diffraction

The technique of resonance X-ray diffraction (Blasie, J.K. and Stamatoff, J. (1981) Annu. Rev. Biophys. Bioeng. 10, 451–452) utilizing synchrotron radiation was used to determine the locations of the cytochrome *c* heme iron atom and the photosynthetic reaction center iron atom within the profile of a reconstituted membrane. The accuracy of these determinations was better than ±2 Å. The cytochrome *c* heme iron atom → reaction center iron atom vector was determined to have a magnitude of approx. 44 Å projected onto the membrane profile and to span most of the lipid hydrocarbon core of the membrane profile. Since the reaction center iron atom interacts magnetically with the primary quinone electron acceptor Q_I over a distance of less than 10 Å, the primary light-induced electron-transfer reactions for this system generate the electric charge separation between oxidized cytochrome c^+ and Fe-Q_I^- across most (approx. 2/3) of the membrane profile including most or all of the lipid hydrocarbon core of the membrane.

Introduction

Current theories concerning the mechanisms of electron-transfer reactions [1–3] and the coupling of these reactions to ATP synthesis [4,5] in biological membranes in general depend critically on the detailed spatial relationships among the various redox centers involved within the membrane structure. Specifically with regard to proposed mechanisms of energy coupling [4,5], the distribution of these redox centers within the membrane profile is of particular significance.

The primary events in bacterial photosynthesis involve light-induced electron-transfer reactions among several redox centers within the reaction center-cytochrome *c* complex in the cytoplasmic membrane of the cell [6–8]. Components known to be involved include a bacteriochlorophyll dimer $(BChl)_2$ which, following light activation, transfers an electron to a bacteriopheophytin (BPh); the bacteriopheophytin then donates an electron to the primary quinone (Q_I). The oxidized $(BChl)_2$ is then rereduced by cytochrome *c*. These early events ultimately generate an electric charge separation

* Present address: Department of Biochemistry, College of Physicians and Surgeons, Columbia University, New York, NY 10032, U.S.A.
** Present address: Celanese Research Company, Summit, NJ 07901, U.S.A.
*** Present address: Exxon Research and Engineering Company, Linden, NJ 07036, U.S.A.

between the net positively charged oxidized cytochrome c^+ electron donor and the net negatively charged reduced primary quinone electron acceptor (Q_I^-) on a microsecond time scale following photon absorption [6–8]. Optical spectroscopy of light-induced carotenoid band-shifts [9] in the cytoplasmic membrane and measurements of light-induced transmembrane electrical currents and potentials [10] in reconstituted membranes have suggested that the cytochrome $c^+ \rightarrow Q_I^-$ charge separation occurs across a large fraction of the membrane profile.

In earlier work [11,12], we have described the reconstitution of a membrane system containing only phospholipid and various reaction center-cytochrome *c* complexes. These reconstituted membranes are essentially unidirectional with regard to the vectorial distribution of reaction center molecules within the membrane profile. The primary photosynthetic events and the orientation of the various chromophores of the complex relative to the membrane plane are identical to those found in the cytoplasmic membrane of the cell. We have utilized X-ray and neutron diffraction techniques to describe fully the separate profile structures of the phospholipid, reaction center and cytochrome *c* molecules within the total profile structure of this reconstituted membrane to approx. 10 Å resolution [11–13].

More recently, we have developed the technique of resonance X-ray diffraction utilizing synchrotron radiation [14] for the determination of the location of the metal atoms associated with redox centers within the membrane structure [15,16]. In this paper, we describe the utilization of resonance X-ray diffraction to determine directly the locations of the cytochrome *c* heme iron atom and the iron atom magnetically coupled with the primary quinone electron acceptor Q_I of the reaction center, within the profile structure of reconstituted membranes containing a reaction center-cytochrome *c* complex.

This work represents the first direct determination of the position and magnitude of the projection of an electron-transfer vector between two (or more) redox centers onto the membrane profile. These studies have been briefly reported elsewhere [17].

Methods

Membrane reconstitution and oriented multilayer preparation

Unilamellar membrane vesicles were reconstituted from egg lecithin and photosynthetic reaction centers as previously described [11]. These vesicles were shown to be essentially unidirectional with regard to the vectorial distribution of reaction center molecules in the membrane profile. Complexes between cytochrome *c* and the reaction centers in these preformed reconstituted membranes were formed via primarily electrostatic interactions as previously described [11]; the cytochrome *c*/reaction center mole ratio was 0.8 for the membranes used in these studies (as determined directly via absorption spectrophotometry of the oriented membrane multilayers). Hydrated oriented multilayers of these fully functional reconstituted membranes were also formed by standard methods described previously [11,12].

Resonance X-ray diffraction methods

The resonance X-ray scattering effects from the iron atom magnetically coupled with the primary quinone electron acceptor Q_I of the reaction center on the first ten orders of lamellar X-ray diffraction from oriented multilayers of reconstituted egg lecithin/reaction center membranes (mole ratio = 100 : 1) were recorded as a function of incident X-ray beam energy over a ± 160 eV range about the measured reaction center iron K-absorption edge using methods already described in considerable detail [15]. These resonance diffraction data were then analyzed via a model refinement analysis which, together with the justification for this type of analysis, has already been described in detail [16]. The determination of the location of the cytochrome *c* heme iron atom within the profile of a reconstituted egg lecithin/reaction center/cytochrome *c* membrane (mole ratio = 100 : 1 : 0.8) via these resonance X-ray diffraction methods has been previously reported by us [16]. The heme iron atom of the cytochrome *c* was chemically replaced by cobalt in these studies so that resonance X-ray scattering from the cobalt atom could be utilized to determine the location of the heme cobalt atom within the membrane profile; this replacement of the cytochrome heme iron

atom by cobalt facilitated the model refinement analysis (i.e., the model refinement analysis requires fewer and less accurate measurements of the resonance scattering effects on the lamellar diffraction the fewer the number of unique resonance scattering atoms in the multilayer unit cell profile).

Results

Our earlier X-ray and neutron diffraction studies have provided directly the separate profile structures of the phospholipid, reaction center and cytochrome *c* molecules within the total profile structure of these reconstituted membranes to approx. 10 Å resolution [11–13]. Some of these profile structures as appropriate to this paper are shown in Fig. 1. These studies demonstrated that minor changes occur within the profile structures of the reaction center molecule and the asymmetric lecithin bilayer upon the primarily electrostatic binding of cytochrome *c* to the reaction center for cytochrome *c*/reaction center mole ratios $\leqslant 1.0$ which are necessary to account completely for the differences in the single membrane profiles shown in Fig. 1a.

Our recently reported resonance X-ray diffraction analysis [15,16] of the location of the cytochrome *c* heme iron (or cobalt) atom in the membrane profile shown in Fig. 1 restricts the heme iron atom location to 61 Å $\leqslant |X| \leqslant$ 64 Å in the half-unit cell (or single-membrane) profile. Since the cytochrome *c* molecule occurs at the very edge of the unit cell profile near $|x| = D/2$ (where D is the multilayer periodicity), two possible interpretations exist for the profiles shown in Fig. 1 concerning the structural interaction of the cytochrome *c* molecule with the reaction center molecule as shown schematically in Fig. 2.

Following our earlier work [15,16], we shall describe the resonance X-ray scattering effects from the iron atom magnetically coupled with the primary quinone electron acceptor Q_I of the reac-

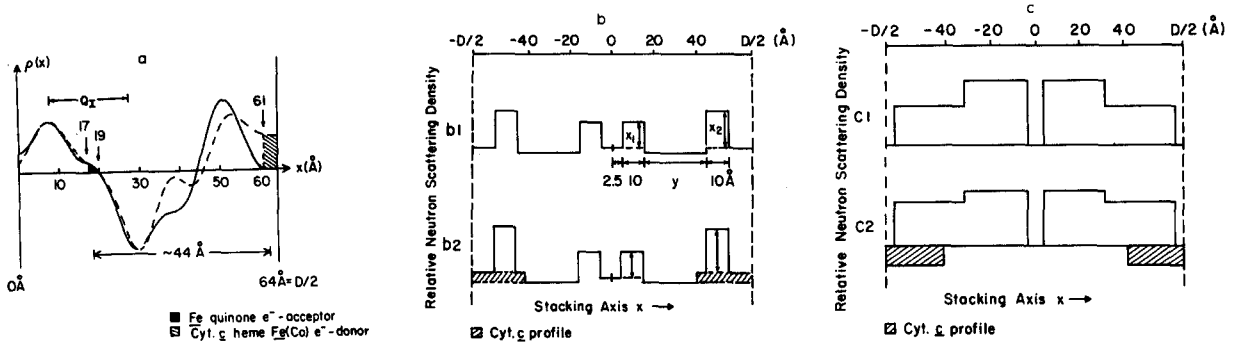

Fig. 1. The combined techniques of X-ray and neutron diffraction have provided [11–13] the separate scattering density profiles for the lecithin, reaction center and cytochrome *c* molecules contributing to the total scattering density profiles of these reconstituted membranes ultimately to approx. 10 Å resolution. (a) The single membrane total electron-density profiles (approx. 10 Å resolution) of the reconstituted lecithin/reaction center (mole ratio = 100 : 1) membrane (solid line) and the reconstituted lecithin/reaction center/cytochrome *c* (mole ratio = 100 : 1 : 0.8) membrane (dashed line). (b) The separate step-function model [11–13] neutron scattering density profiles of the lecithin molecules contributing to the lecithin/reaction center membrane profile (b1) where $x1 : x2 = 0.7$ and $y = 32$ Å and the lecithin/reaction center/cytochrome *c* membrane profile (b2) where $x1 : x2 = 0.9$ and $y = 33$ Å as refined from approx. 30 Å resolution data. The lecithin bilayer is somewhat less asymmetric when cytochrome *c* is electrostatically bound to the reaction centers. The position of the refined step-function model profile of cytochrome *c* within the single-membrane profile is also indicated. (c) The separate step-function model [11–13] neutron scattering density profiles of the reaction center molecules contributing to the lecithin/reaction center membrane profile (c1) and the lecithin/reaction center/cytochrome *c* membrane profile (c2) as refined from approx. 30 Å resolution data. These two reaction center profiles exhibit small, but experimentally significant differences. The position of the refined step-function model profile of cytochrome *c* within the single-membrane profile is also indicated. The location of the cytochrome *c* heme iron atom at $|X| \simeq 62.5 \pm 1.5$ Å, as determined by the resonance X-ray diffraction analysis reported in this paper, is indicated in the lecithin/reaction center/cytochrome *c* membrane electron-density profile shown in panel a. The location of the iron atom magnetically coupled with the primary quinone electron acceptor of the reaction center at $|X| \simeq 18 \pm 1$ Å, as also determined by the resonance X-ray diffraction analysis reported in this paper, is indicated in both of the total electron-density profiles shown in panel a. Q_I must be located within 10 Å of the reaction center iron atom due to the prominence of the magnetic coupling; therefore, Q_I is located in these single-membrane profiles within the region indicated in panel a, namely, $|X| \simeq 18 \pm 10$ Å.

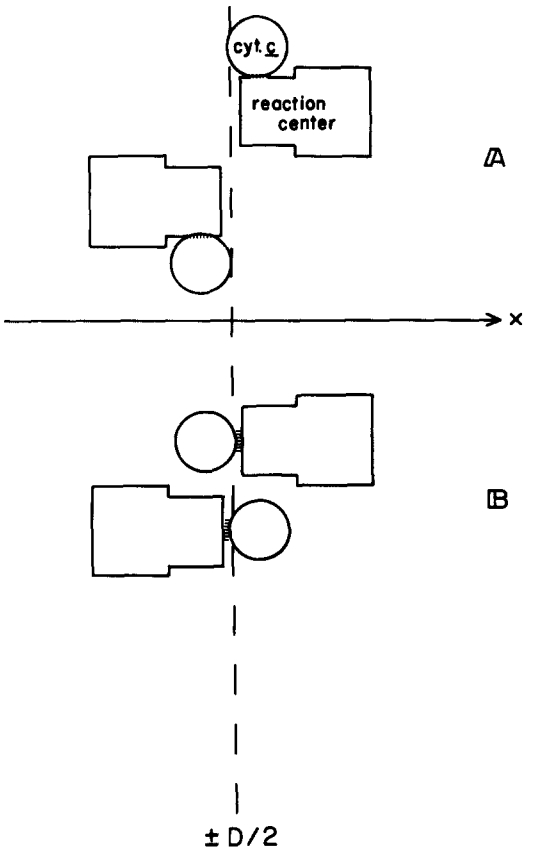

Fig. 2. Schematic representations of the two possible modes of electrostatic binding of cytochrome *c* molecules in these reconstituted membranes which are consistent with the profiles shown in Fig. 1. These two possibilities arise because of the mirror plane of symmetry in the multilayer unit cell profile at $|X| = D/2$ and the location of the cytochrome *c* molecules at the edge of the unit cell profile adjacent to $|X| = D/2$. These representations are only approximately to scale in terms of the available structural data (see Fig. 5 for details) and hold only for cytochrome *c*/reaction center mole ratios of $\leqslant 1.0$.

tion center on the lamellar X-ray diffraction from oriented multilayers of reconstituted lecithin/reaction center membranes in terms of differential resonance scattering effects $R_e(h/h')$ where:

$$R_e(h/h') \equiv \left(\frac{|F_{E2}(h)|^2}{|F_{E2}(h')|^2} - \frac{|F_{E1}(h)|^2}{|F_{E1}(h')|^2} \right) \Big/ \left(\frac{|F_{E2}(h)|^2}{|F_{E2}(h')|^2} \right)$$

and $F_E(h)$ is the structure factor for the hth order lamellar reflection at incident X-ray beam energy E where $E2$ is 'far' from an absorption edge and $E1$ is the absorption edge energy. In Fig. 3, we show the ratios $|F_E(h)|^2/|F_E(h')|^2$ for (h/h') values of (3/2), (4/2), (6/2) and (8/2) and $E2$ values of ± 160, ± 80 and ± 40 eV with respect to the reaction center iron K-absorption edge $E1$. We note that the dependence of these ratios on incident beam energy is dominated by the real part of the resonant component of the iron atomic scattering factor, f', for these multilayers (see Eqn. 8 of Ref. 15). As a result, the energy dependence of these ratios as measured is consistent with an appropriate Hilbert transform of the measured reaction center iron K-edge absorption spectrum, noting the relatively low resolution of our incident beam energy scans ($\Delta E \simeq 40$ eV with an incident beam bandwidth of approx 2 eV). From Fig. 3, the signs of the differential scattering effects are clearly negative for $R_e(3/2)$ and $R_e(4/2)$ and positive for $R_e(6/2)$ and $R_e(8/2)$. These particular $R_e(h/h')$ values of those measured have smaller experimental errors for the several reasons described in detail in our earlier work [15].

These more accurate differential resonance scattering effects obtained from Fig. 3 were then subjected to a model refinement analysis as described in detail previously [16]. This analysis utilized the known phased profile structure of this lecithin/reaction center membrane [11,12] together with the experimentally determined virtually unidirectional nature of the vectorial distribution of reaction center molecules in this membrane profile [11]. The latter fact implies that there is only one unique reaction center iron atom location in the single-membrane profile. The calculated differential resonance scattering effects $R_c(h/h'; X)$ (see Ref. 16 for further details) as a function of the position $|X|$ of the one unique reaction center iron atom in the half-unit cell (or single-membrane) profile for $h' = 2$ and $h = 3$, 4, 6 and 8 are shown in Fig. 4. A comparison of these calculated $R_c(h/h'; X)$ functions with only the signs of the measured $R_e(h/h')$ effects for $h' = 2$ and $h = 3$, 4, 6 and 8 can readily be seen to be sufficient to restrict the position of the one unique reaction center iron atom to 17 Å $\leqslant |X| \leqslant$ 19 Å within the single-membrane profile as shown in Fig. 1. In addition, the relative magnitudes of the calculated differential resonance scattering effects $R_c(h/h'$; 17 Å $\leqslant |X| \leqslant$ 19 Å) agree reasonably well with the measured differential scattering effects $R_e(h/h')$ (see Ref. 16 for further details).

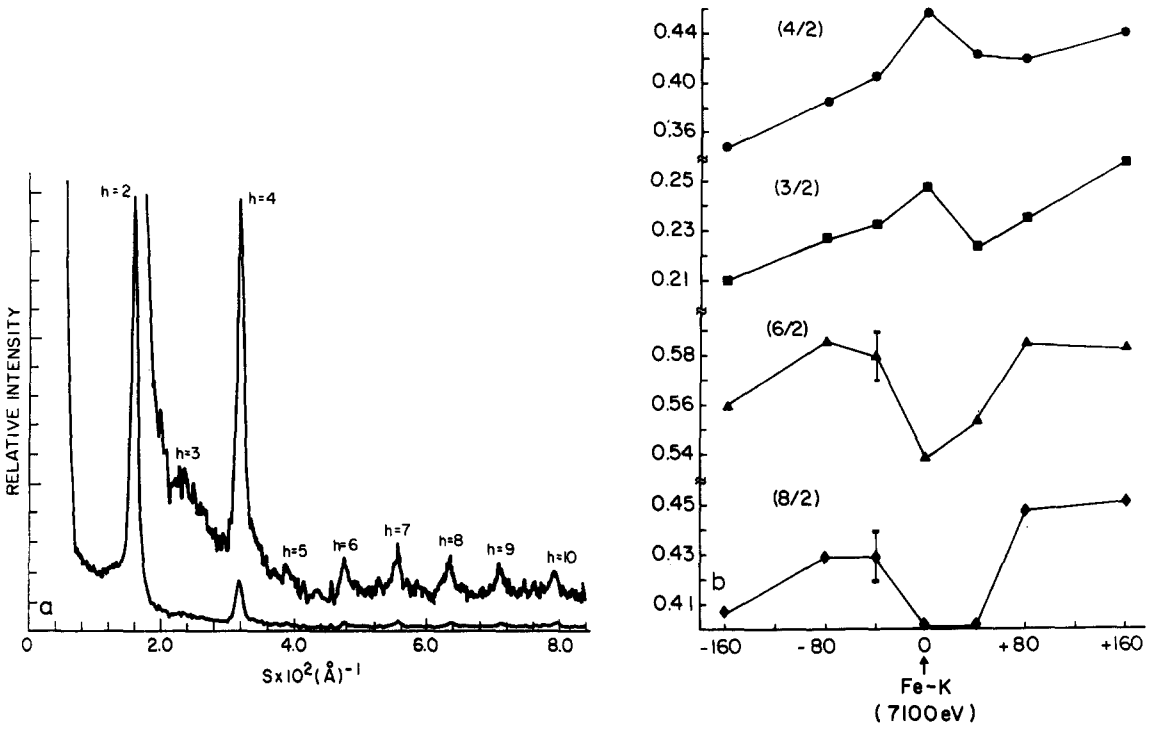

Fig. 3. The lamellar X-ray diffraction (a) from an oriented multilayer of reconstituted lecithin/reaction center membranes collected on a focused beam-line at the Stanford Synchrotron Radiation Laboratory using $\theta-2\theta$ scans, 1-s data collection per θ value and a monochromatic bandwidth of less than 5 eV (see Ref. 15 for details). Such $\theta-2\theta$ scans collected at appropriate incident X-ray energies provided the measured differential resonance X-ray scattering effects $R_e(h/h')$ from the iron atom magnetically coupled with the primary quinone electron acceptor of the reaction center on the various lamellar reflections from the oriented multilayer of reconstituted lecithin/reaction center membranes (mole ratio = 100 : 1). The ratios $|F_E(h)|^2/|F_E(h')|^2$ for $h' = 2$ and $h = 3$, 4, 6 and 8 and $E2$ values of ± 160, ± 80 and ± 40 eV with respect to the reaction center iron K-edge $E1$ at 7100 eV are shown in panel b. See text and Ref. 15 for further details.

Discussion

The results of our resonance X-ray diffraction analysis clearly indicate that the iron atom magnetically coupled with the primary quinone electron acceptor Q_I of the reaction center is located within the narrow region 17 Å $\leqslant |X| \leqslant$ 19 Å of the single-membrane profile. Our earlier results [15,16] clearly indicated that the heme iron (or cobalt) atom of cytochrome *c* electrostatically bound to the reaction center is located within the narrow region 61 Å $\leqslant |X| \leqslant$ 64 Å of the single-membrane profile for cytochrome *c*/reaction center mole ratios $\leqslant$ 1.0. Given the close similarity of the reaction center profile structure within the profile structures of these reconstituted lecithin/reaction center and lecithin/reaction center/cytochrome *c* membranes as determined independently [11–13], these results indicate that the projection of the vector between the cytochrome *c* heme iron atom and the iron atom magnetically coupled with the reaction center primary quinone electron acceptor Q_I onto the single-membrane profile extends from $|X| \simeq 62.5 \pm 1.5$ Å * to $|X| \simeq 18.0 \pm 1.0$ Å within

* We note that the alternative mode of electrostatic binding of cytochrome *c* to the reaction center (case B, Fig. 2) would place the relevant (electron donor) cytochrome *c* heme iron atom at $|X| \simeq 65.5 \pm 1.5$ Å within the single-membrane profile. Since this alternative result has only a negligible effect on the following discussion and since we favor the mode of cytochrome *c* binding given in case A, Fig. 2 (based on the behavior of the unit cell electron-density profiles near $|X| \simeq D/2$ at a resolution of 10 Å for cytochrome *c*/reaction center mole ratios ranging from 0 to 3), we have excluded consideration of this alternative mode of cytochrome *c* binding from further discussion.

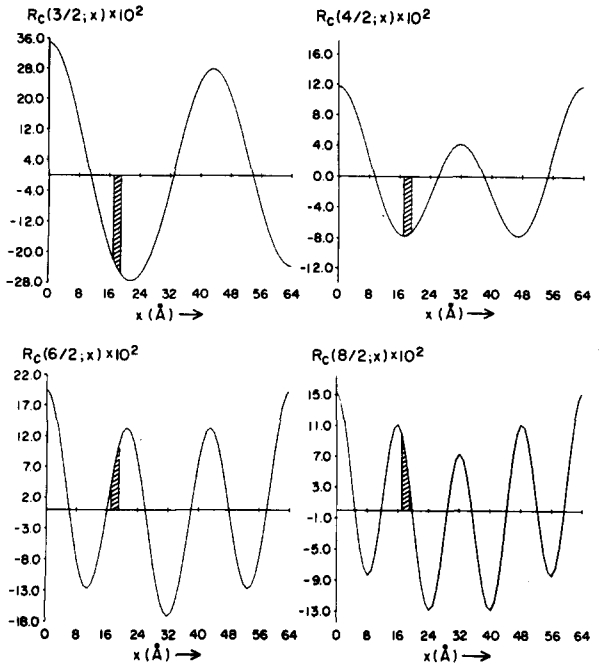

Fig. 4. The calculated differential resonance scattering effects $R_c(h/h';X)$ as a function of the position $|X|$ of the one unique reaction center iron atom in the single-membrane profile for $h'=2$ and $h=3$, 4, 6 and 8. It can readily be seen that agreement between only the signs of the measured differential effects (which are clearly negative for $R_e(3/2)$ and $R_e(4/2)$ and positive for $R_e(6/2)$ and $R_e(8/2)$ from Fig. 3) and the calculated differential effects $R_c(h/h';X)$ can be achieved only within the one narrow region 17 Å $\leq |X| \leq$ 19 Å of the single-membrane profile. See text and Ref. 16 for further details.

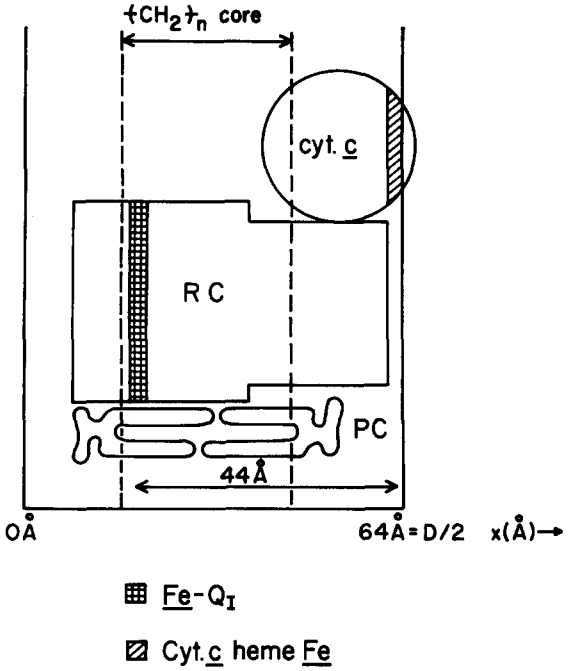

Fig. 5. A schematic representation to scale of our current knowledge concerning the structure of the cytochrome *c*-reaction center (RC) complex incorporated into the lipid (PC, phosphatidylcholine) bilayer of these reconstituted membranes (for cytochrome *c*/reaction center mole ratios $\leq$ 1.0). The positions of the cytochrome *c* heme iron atom electron donor and the iron atom of the reaction center Fe-Q_I primary quinone electron acceptor within the profile structure of the complex are indicated as determined by the resonance X-ray diffraction experiments.

the single-membrane profile. Hence, the projection of this electron-transfer vector onto the membrane profile representing the primary electric charge separation resulting from photon absorption (i.e., cytochrome $c^+ \rightarrow$ Fe-Q_I^-) has a magnitude of approx. 44 ± 2 Å (approx. 2/3 of the single-membrane profile whose extent is approx. 64 Å) and spans most of the lipid hydrocarbon core of the membrane profile (which extends from $|X| \approx 15$ Å to $|X| \approx 45$ Å in the single-membrane profile). The reader should refer to Fig. 1 for illustration of the above points.

We note that the electron involved in this primary charge separation actually resides on the primary quinone molecule Q_I. It is now well established that the reaction center high-spin ferrous iron atom is magnetically coupled with Q_I as the semiquinone (Q_I^-) (see Ref. 18 for reviews). While the exact nature of the magnetic interaction is not yet understood [19], thereby making it impossible to make an accurate distance measurement between the paramagnetic centers, the prominence of the magnetic interaction would indicate a distance of less than 10 Å. Therefore, this electron-transfer vector projected onto the membrane profile could possibly be in error by as much as ± 10 Å depending critically on the orientation of the Fe-Q_I vector relative to the membrane plane. These limits on the position of Q_I in the membrane profile are indicated in Fig. 1. Structural studies of the location of Q_I itself within these membrane profiles are currently underway in our laboratories.

These results described above have strong im-

plications for the possible mechanisms of the electron-transfer reactions generating the primary electric charge separation between oxidized cytochrome c^+ and Fe-Q_I^-. If significant overlap of molecular orbitals between successive elements of this light-induced electron-transfer process exists, the known elements intervening between cytochrome *c* and the primary quinone electron acceptor Q_I (namely, the bacteriochlorophyll dimer, the bacteriochlorophyll monomer and the bacteriopheophytin monomer [6–8,20]) would have to be arranged approximately linearly across the membrane profile within the region 18 Å $\leqslant |X| \leqslant$ 62.5 Å with the planes of their conjugated rings oriented approximately perpendicular to the membrane plane. In addition, Q_I would have to be located within the region 18 Å $\leqslant |X| \leqslant$ 28 Å of the membrane profile. Hence, vibronically coupled electron tunneling between these redox centers [2,3] could indeed occur, but perhaps only under the set of structural considerations described above. A number of less direct measurements suggest that these structural requirements could be met: (a) EPR and optical linear dichroism studies of these oriented multilayers have suggested that the conjugated rings of the bacteriochlorophyll dimer, Q_I and the bacteriopheophytin monomer could be oriented approximately perpendicular to the membrane plane [21]; (b) EPR studies [22,23] and kinetic measurements [24] have suggested that the distance between Q_I and its electron donor bacteroipheophytin is about 9–12 Å; (c) pulsed-EPR methods [25] have indicated a distance of 12–17 Å between the reaction center iron atom and the bacteriochlorophyll dimer; (d) electric potential measurements in vivo [26] and on planar reaction center/cytochrome *c* reconstituted membranes [10] have indicated that a similar 'dielectric distance' exists between the $(BChl)_2$ and Q_I and between the cytochrome *c* heme and the $(BChl)_2$ in the membrane profile and; (e) EPR measurements on *Rhodopseudomonas sphaeroides* and *Chromatium vinosum* have suggested center-center distances of greater than 25 Å between the cytochrome *c* heme and the $(BChl)_2$ [27] and greater than 23 Å between Q_I and the $(BChl)_2$ [27–29]. Structural studies concerning the direct location of these intervening elements of the light-induced electron-transfer process within the membrane profile would be highly desirable.

With regard to current theories concerning energy-coupling mechanisms, it is clear from these studies that the light-induced electric charge separation between oxidized cytochrome c^+ and Fe-Q_I^- occurs across virtually all of the lipid hydrocarbon core of this membrane profile. As a result, this light-induced primary electric charge separation resulting from a series of electron-transfer steps between cytochrome *c* and Q_I can directly generate of the order of 50–100 mV transmembrane electric potential within microseconds of photon absorption under single-turnover conditions, i.e., one photon absorbed per reaction center, assuming a reasonable value for the membrane capacitance of the order of 1 $\mu F/cm^2$ [10] and a reaction center density in the plane of the natural membrane of approx. $2 \cdot 10^{11}/cm^2$ [10].

The results of these and our earlier studies may be summarized schematically in Fig. 5. We note that these resonance X-ray diffraction studies represent the first direct determination of the position and magnitude of the projection of an electron-transfer vector between two redox centers onto the membrane profile.

References

1 Chance, B., DeVault, D., Frauenfelder, H., Marcus, R., Schrieffer, R. and Sutin, N. (1979) Tunneling in Biological Reactions, Academic Press, New York
2 Hopfield, J.J. (1974) Proc. Natl. Sci. U.S.A. 71, 3640–3644
3 Jortner, J. (1976) J. Chem. Phys. 64, 4860–4867
4 Mitchell, P. (1976) J. Theor. Biol. 62, 327–367
5 Dutton, P.L. and Prince, R.C. (1978) The Bacteria 6, 523–584
6 Dutton, P.L., Prince, R.C. and Tiede, D.M. (1972) Photochem. Photobiol. 28, 939–949
7 Blankenship, R.E. and Parson, W.W. (1979) in Photosynthesis in Relation to Model Systems (Barber, J., ed.), pp. 71–114, Elsevier/North-Holland, Amsterdam
8 Feher, G. and Okamura, M.Y. (1976) Brookhaven Symp. Biol. 28, 183–194
9 Jackson, J.B. and Dutton, P.L. (1973) Biochim. Biophys. Acta 325, 102–113
10 Packham, N.K., Dutton, P.L. and Mueller, P. (1982) Biophys. J. 37, 465–473
11 Pachence, J.M., Dutton, P.L. and Blasie, J.K. (1979) Biochim. Biophys. Acta 548, 348–373
12 Pachence, J.M., Dutton, P.L. and Blasie, J.K. (1981) Biochim. Biophys. Acta 635, 267–283

13 Pachence, J.M., Dutton, P.L. and Blasie, J.K. (1983) Biochim. Biophys. Acta 724, in the press
14 Blasie, J.K. and Stamatoff, J. (1981) Annu. Rev. Biophys. Bioeng. 10, 451–452
15 Stamatoff, J. Eisenberger, P. Blasie, J.K., Pachence, J.M., Tavormina, A., Erecinska, M., Dutton, P.L. and Brown, G. (1982) Biochim. Biophys. Acta 679, 177–187
16 Blasie, J.K., Pachence, J.M., Tavormina, A., Erecinska, M., Dutton, P.L., Stamatoff, J., Eisenberger, P. and Brown, G. (1982) Biochim. Biophys. Acta 679, 188–197
17 Blasie, J.K., Pachence, J.M., Dutton, P.L., Stamatoff, J., Eisenberger, P. and Brown, G. (1982) Biophys. J. 37, 149a.
18 Sistrom, W.R. and Clayton, R.K. (1978) The Photosynthetic Bacteria, Plenum Press, New York
19 Bulter, W.F., Johnston, D.C., Shore, H.B., Fredkin, D.R., Okamura, M.Y. and Feher, G. (1980) Biophys. J. 32, 967–992
20 Parson, W.W. (1982) Annu. Rev. Biophys. Bioeng. 11, 57–80
21 Tiede, D.M. and Dutton, P.L. (1981) Biochim. Biophys. Acta 637, 278–290
22 Tiede, D.M., Prince, R.C. and Dutton, P.L. (1976) Biochim. Biophys. Acta 449, 447–469
23 Okamura, M.Y., Isaacson, R.A. and Feher, G. (1979) Biochim. Biophys. Acta 546, 394–417
24 Peters, K., Avouris, P. and Rentzepis, P.M. (1978) Biophys. J. 23, 207–217
25 Norris, J.R., Thurndur, M.C. and Bowman, M.K. (1980) Adv. Biol. Med. Phys. 17, 365–416
26 Takamiya, K. and Dutton, P.L. (1977) FEBS Lett. 80, 279–284
27 Tiede, D.M., Leigh, J.S. and Dutton, P.L. (1978) Biochim. Biophys. Acta 503, 524–544
28 Tiede, D.M., Leigh, J.S. and Dutton, P.L. (1978) in Frontiers in Bioenergetics (Dutton, P.L., Leigh, J.S. and Scarpa, A., eds.), pp. 45–53, Academic Press, New York
29 McElroy, J.D., Feher, G. and Mauzerall, D.C. (1972) Biochim. Biophys. Acta 267, 363–374